To the Graduate Council:

I am submitting herewith a thesis written by Douglas F. Britton entitled "A Refractive Technique For Surface Flow Visualization Using Image Processing." I have examined the final copy of this thesis for form and content and recommend that it be accepted in partial fulfillment of the requirements for the degree of Master of Science, with major in Electrical Engineering.

Dr. Montgomery Smith, Major Professor

We have read this thesis
and recommend its acceptance:

Accepted for the council:

Associate Vice Chancellor
and Dean of the Graduate School

STATEMENT OF PERMISSION TO USE

In presenting this thesis in partial fulfillment of the requirement for a Master's degree at The University of Tennessee, Knoxville, I agree that the Library shall make it available to borrowers under rules of the Library. Brief quotations from this thesis are allowable without special permission, provided that accurate acknowledgment of the source is made.

Permission for extensive quotation from or reproduction of this thesis may be granted by my major professor, or in his absence, by the Head of Interlibrary Services when, in the opinion of either, the proposed use of the material is for scholarly purposes. Any copying or use of the material in this thesis for financial gain shall not be allowed without my written permission.

Signature Douglas F. Britton

Date April 28, 1994

A REFRACTIVE TECHNIQUE FOR SURFACE FLOW VISUALIZATION USING IMAGE PROCESSING

A Thesis

Presented for the

Master of Science

Degree

The University of Tennessee, Knoxville

Douglas F. Britton

May 1994

ACKNOWLEDGMENTS

I would like to express my appreciation to Dr. Montgomery Smith, who served as the chairman of the committee, for his classes, help, guidance, and advice concerning this thesis. I would like to express my thanks to Dr. Bruce Bomar, who served as a committee member, for his helpful classes and guidance. Special thanks to Dr. Ahmad Vakili, who also served on the committee, for his assistance in the experimental phase of this thesis.

I would like to thank my parents and family for their encouragement and prayer support these last two years. Finally, to God be the glory for the great things He has done.

ABSTRACT

The wake/free surface interaction has become a major research topic in the field of hydrodynamics with special applications in the detection, classification, and tracking of submerged objects. This has led to the development of a simple but effective free surface visualization technique which can be implemented in controlled water tunnel experiments. An experiment was performed to verify the effectiveness and applicability of this method.

Digital images of a spatially varying cosine grid were acquired as seen through the disturbance pattern present on the water surface. Image processing techniques were used to perform phase demodulation of the distorted image by cross-multiplying the data image with a reference image and then low pass filtering the result. Contrast stretching was performed to enhance the subjective quality of the contents in the final image. The resulting product of the process is an image which details the outline, location, and extent of the surface deformation in a grayscale format. Optimal digital filters and spatial cosine grids are determined experimentally for various surface flow conditions.

TABLE OF CONTENTS

CHAPTER PAGE

I. INTRODUCTION 1

II. THEORY 6

Refraction of Light by Water 6

Mathematical Derivation 8

Filter Design and Implementation 10

III. PRACTICAL IMPLEMENTATION 13

Experimental Setup 13

Reconstruction Method 16

IV. RESULTS AND ANALYSIS 21

Water Droplet Data 21

Wake Flow Surface Disturbance 26

V. SUMMARY AND CONCLUSIONS 30

BIBLIOGRAPHY 33

APPENDIXES 36

A. FORTRAN CODE FOR THE CROSS MULTIPLICATION 37

B. FORTRAN CODE FOR THE FILTER PROCEDURE 40

VITA 48

LIST OF FIGURES

FIGURE PAGE

2.1. 3-D form of Snell's Law. 6

3.1. Physical layout of the experiment. 14

3.2. General block diagram of the reconstruction process. 20

4.1. Reference image using a 2.5 cycle/cm cosine grid. 22

4.2. Data image of a water droplet using a 2.5 cycle/cm cosine grid. 22

4.3. Cross-multiplication of the reference image (Figure 4.1) and the data image (Figure 4.2). 23

4.4. The filtered cross-multiplication image in Figure 4.3. 23

4.5. Filtered image after contrast stretching (110 to 140). 24

4.6. Wave flow surface using a 2.5 cycle/cm cosine grid. 27

4.7. Wake flow surface using a 1.04 cycle/cm cosine grid. 27

4.8. Wake flow surface using a 0.83 cycle/cm cosine grid. 28

CHAPTER I

INTRODUCTION

The study of the wake/free surface relationship has become increasingly more important in the detection, classification, and tracking of submerged objects. As a result, it has become a major research topic in the field of hydrodynamics. The ability to understand the causes and interactive forces which contribute to prolonged free surface turbulence has resulted in the development of new free surface visualization techniques [1]. The objective of this work has been to develop a new technique to visualize the surface height variation in a water tunnel using image and signal processing methods.

Most of the previous flow visualization techniques (hydrogen bubble, fluorescent die injection, particle injection, etc.) [2,3,4] were concerned with visualizing subsurface characteristics of the flow. Several techniques [5,6,7,8,9] have been presented which allow the visualization of disturbances on the free surface. Any method which would require a physical interaction with the flow is highly undesirable because it would alter the flow. As a result, most modern visualization techniques employ optical methods and some type of image processing since these do not disturb the flow.

Cox [10] implemented a technique by which he measured the free surface slope using the refraction of light through the free surface. One point on the water was illuminated from below the flow into a photocell using a telescope and a light source of spatially-linear varying intensity. A relationship was then established

between the intensity of the light recorded by the photocell and one component of the free surface slope. This method is commonly know as the "refractive method" [8]. Sorrell and Withers [11] implemented a discrete system using an array of photovoltaic cells to measure the refraction of the light ray in one dimension. Outputs from the photocells were converted to TTL levels and then run through comparators to determine the active status. This enabled them to trace the location of the refracted light ray.

A different technique known as the "reflective method" allows observation of the free surface by illuminating the water from above. The surface deformation information is then acquired from the light reflecting off the free surface [8]. Gotwols and Irani [7] implemented the reflective method by using a charge-coupled device (CCD) camera to obtain images of ocean gravity waves. They then took the 2-D and 3-D Fourier transforms to obtain the direction wave number spectrum and the wave number-frequency spectrum. Sarpkaya and Henderson [12] analyzed free surface scars and striations due to trailing vortices by taking images of the shadows of the surface disturbances. Dabiri, Zhang, and Gharib [8] developed a method to allow real time mapping of the free surface deformation. Their method uses a sheet of different colored parallel light rays to illuminate the surface. The result is a color coded image of the surface slopes. The image is analyzed in the hue, saturation, and intensity (HSI) domain using image processing techniques. The surface elevation is calculated using Fourier mathematics and mapped into a surface plot.

Moire techniques function by casting a shadow of a grid or grating on the

free-surface from above. Then by imaging the shadow and using image processing and geometric techniques, a grayscale image of the surface is generated. Grant, Padilla, and Stewart [6] used the projection Moire method to simulate the upwelling phenomenon arising from the interaction of incident waves with large diameter blocked structures. A very narrowly spaced grid was projected on the water surface, while matched optics in the camera were used to generate the Moire fringes. The result was an image of coarse fringes representing surface contours overlaid on an image of the water surface. Mizuno, Nagese, and Yamauchi [9] developed the K. Moire method which allows visualization of disturbances which are in the x-y plane of the fluid.

The problem with most of the current surface visualization techniques is that they require elaborate and costly experimental configurations which need precise calibration. One of the difficulties with the reflective method is the transparency of the water [6]. The Moire techniques require the use of two identical high quality grids which must be carefully aligned in order to produce the proper interference or Moire fringes.

The surface disturbance visualization method presented in this thesis is a simple but effective method for obtaining experimental surface deformation data in a water tunnel. This is a refractive method which takes advantage of the light "bending" characteristics of water. A spatially-varying cosine grid was located on the bottom surface of a water tunnel. A disturbance on the free surface "bent" the lines of the cosine grid thus producing a phase modulated sinusoidal pattern. Images

of the distorted cosine grid (which will be referred to as the data images) were acquired in ambient light from above the free surface by a video camera input to a framegrabber. The bending of the cosine grid was assumed to be a phase shift or modulation of the original cosine. Each row of the data image was then cross-multiplied with a corresponding row in an image of the undisturbed flow (which will be referred to as the reference image). This cross multiplication isolated the phase information in the low end of the frequency spectrum. A digital low pass filter (LPF) was then used to reject the high frequency components and pass only the surface disturbance information which was contained in the phase. Image enhancement techniques were then used to emphasize the desired information in the image and minimize the unwanted information.

This technique has proven to be an effective method of visualizing the free surface turbulence in a water tunnel where the turbulence is mild. The grayscale image which results has dark sections which represent the surface disturbance on a gray background. Five different spatial cosine grids (each with a different frequency) were used to determine experimentally the optimal grid frequency. The higher frequency grids resulted in higher resolution images of the disturbance, while it was easier to filter out the cosine in the mid-range frequencies. It was very difficult to filter out the low frequency cosine grids without affecting the data in the image.

The theoretical aspects of this technique are explained in greater detail in Chapter II. Included in the discussion are the design requirements of the digital

LPF. In Chapter III, a description of the experimental procedure is presented. A number of different experiments were performed using different cosine grids. This was done to determine experimentally the optimal design parameters for this technique. Chapter IV presents the results and analysis of this technique. Images in the various steps in the process are displayed and explained. A comparison is made between the images acquired using the different frequency cosine grids.

CHAPTER II

THEORY

Refraction of Light by Water

This method takes advantage of the light refraction characteristics of water as they affect the image of the bottom of a tank or water tunnel. Light rays emanating from the tunnel bottom pass through the water surface and are observed from above. Figure 2.1 details the physics principles behind a refractive technique.

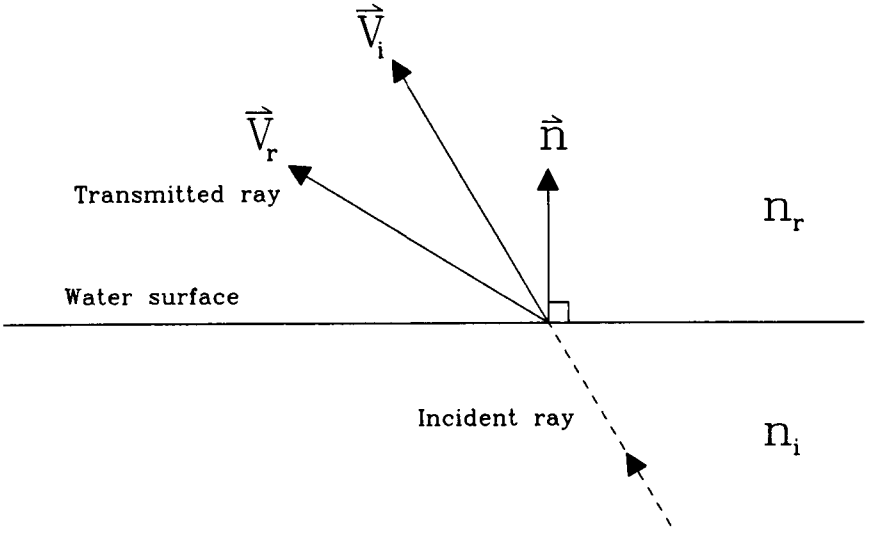


Figure 2.1: 3-D form of Snell's Law.

The three-dimensional form of the law of refraction, better known as Snell's law [13], is given as

$$n_i \overline{V}_i \times \overline{n} = n_r \overline{V}_r \times \overline{n} \quad , \tag{2.1}$$

where n_i and n_r are the indices of refraction for the materials in which the incident ray with direction vector $\overline{V}_i$ and the refracted ray with direction vector $\overline{V}_r$ are present. In this case n_i would be the index of refraction of water, while n_r would be the index of refraction of air. The vector $\overline{n}$ represents the unit normal to the water surface and is defined as

$$\overline{n} = \frac{1}{\sqrt{\left(\frac{\partial s}{\partial x}\right)^2 + \left(\frac{\partial s}{\partial x}\right)^2 + 1}} \begin{bmatrix} -\frac{\partial s}{\partial x} \\ -\frac{\partial s}{\partial y} \\ 1 \end{bmatrix} , \tag{2.2}$$

where s is the surface defined by the function

$$z = s(x,y) \quad . \tag{2.3}$$

Light rays directed vertically through the water perpendicular to a quiescent surface would penetrate without being refracted. However, if the surface were turbulent, the light rays penetrating the surface would be refracted in different directions. For small surface deformations, where

$$\left|\frac{\partial s}{\partial x}\right|, \left|\frac{\partial s}{\partial y}\right| < 1 \quad , \tag{2.4}$$

the resulting image of the water tunnel bottom is a warped or distorted version of any pattern on the bottom.

Mathematical Derivation

The objective of this technique is to visualize the free surface outline in the form of a grayscale image. This is accomplished by placing a two-dimensional sinusoidal pattern on the bottom of the tunnel. With a quiescent water surface, the resulting ideal digitized intensity image (or reference image) is given by

$$I_r(m,n) = A_r + B_r Cos(\omega_o m + \phi_o) \quad , \tag{2.5}$$

where ω_o is the spatial frequency of the cosine and m and n denote the spatial coordinates of the image. With a mild disturbance at the free surface, the resulting digitized intensity image (or data image) is given as

$$I_d(m,n) = A_d + B_d Cos(\omega_o m + \phi_o + \phi(m,n)) \quad , \tag{2.6}$$

where $\phi(m,n)$ contains the information about the water surface disturbance pattern.

If the surface disturbance becomes too severe, the light penetrating the water surface could scatter too much resulting in a loss of intensity. Such conditions could also

result in the crossing of the grid lines or breakup. The ϕ_o takes into account any initial phase offset of the image. It is the same for both the reference and data images. With the constant background dc components removed, the images can be cross-multiplied to obtain

$$f(m,n) = \left[I_r(m,n) - A_r\right]\left[I_d(m,n) - A_d\right] \tag{2.7}$$

$$= B_r B_d Cos(\omega_o m + \phi_o) Cos(\omega_o m + \phi_o + \phi(m,n)) \tag{2.8}$$

$$= \frac{B_r B_d}{2} Cos[\phi(m,n)] + \frac{B_r B_d}{2} Cos[2\omega_o m + 2\phi_o + \phi(m,n)] \quad . \tag{2.9}$$

The higher frequency components centered at $2\omega_o$ can be removed by lowpass filtering the image to yield

$$g(m,n) = \frac{B_r B_d}{2} Cos[\phi(m,n)] \quad . \tag{2.10}$$

The filtered image can be scaled and a constant added to produce a final processed intensity image given by

$$I_p(m,n) = A_p + B_p\, Cos[\phi(m,n)] \quad . \tag{2.11}$$

This is the process by which the spatial two-dimensional extent and shape of the water surface causing the phase shift $\phi(m,n)$ produces an image with observable

intensity variations. The method for implementing this process is discussed in Chapter III. It should be noted that the reference phase ϕ_o can vary with position as long as it remains the same for both the reference and data images. As a result, the initial alignment of the grid is not critical. The grid, however, should be sinusoidal to avoid harmonics and thus ensure that the higher frequencies are centered at $2\omega_o$.

Filter Design and Implementation

All of the image processing, including the filtering, is performed row by row as a function of the index m . The cross-multiplied image contains frequency components at both zero and $2\omega_o$, so the cutoff frequency for the LPF should be approximately half way between the two at around ω_o . A practical objective for the LPF is to reduce the amplitude of the higher frequency components to less than the maximum value of the quantization error in the final image. Since the frequency components at zero and $2\omega_o$ have approximately the same energy, the stopband

attenuation and the passband ripple should be such that

$$\delta_1 = \delta_2 = \frac{1}{L} \quad , \tag{2.12}$$

where L is the total number of gray levels possible in the final displayed image.

In order to preserve the locations and extent of the artifacts in the images, the filters must have zero-phase responses. The design of optimal min-max or equiripple finite impulse response (FIR) filters can be accomplished using the Parks-McClellan program [14,15]. In the design process the user specifies the desired number of filter coefficients or taps, the passband and stopband ranges, and the weighting factors desired in each band. Using an iterative process, the Parks-McClellan program generates a set of filter coefficients which has an equiripple frequency response with minimal error at the extrema frequencies [14,15]. The design parameters are adjusted until the frequency response of the resulting filter meets the desired ripple specifications for each band. This program produces linear phase FIR filters by constraining the impulse response to be symmetric. A zero phase filter can be achieved by specifying an odd number of filter taps and shifting the point of symmetry to the origin. The filter design specifications used in the actual implementation are discussed in Chapter III.

Digital filters can be implemented either by convolving the data with the filter coefficients in the spatial domain or by multiplying the Fourier transforms of the data and the filter coefficients in the frequency domain. In the latter case, the

discrete Fourier transform (DFT) is taken of both the data sequence and the filter coefficients by means of the fast Fourier transform (FFT). Prior to taking the FFT, the filter coefficient sequence is zero padded until its length is equal to that of the data sequence. Once the FFT's have been taken they are cross-multiplied, and the inverse fast Fourier transform (IFFT) is taken to return the resulting filtered data sequence. Since circular convolution is the spatial domain dual of DFT frequency domain multiplication, circular convolution effects are present in the first and last ½(M-1) filtered data points, where M is the length of the nonzero filter coefficient sequence. As a result, these points are erroneous and should not be considered during evaluation of the filtered data sequence.

CHAPTER III

PRACTICAL IMPLEMENTATION

Experimental Setup

In order to test the effectiveness of this method, an experiment was designed and implemented using a low turbulence water tunnel. The flow channel of the tunnel was 38 cm wide, 137 cm long, and 30 cm deep. There was no top on the open section of the tunnel. The two remaining sides and bottom consisted of transparent high strength plexi-glass. This allowed plenty of ambient light to penetrate the water, reflect off the grid placed on the bottom, and refract at the surface. It also made changing the spatial cosine grid simple, since it was fastened to the underside of the tunnel. The lighting in the water tunnel test facility consisted of the overhead fluorescent lights and a 300 Watt dispersed white light.

The data acquisition equipment included a monochrome 512 by 512 CID video camera which was mounted on an adjustable rack directly above the flow channel. A zoom lens (10X, 10.5-105 mm) was used to observe the flow. The camera and lens were configured so that the cosine grid as seen through the water filled the entire field of view. The aperture of the lens was set to allow the viewing of a maximum contrast between black and white sections on the grid without blurring or distorting the quality of the image. The output from the camera was connected directly to a framegrabber card mounted in a 486-PC host computer. The output from the framegrabber was then shown on a Sony Trinitron RGB monitor.

All of the frames were stored digitally on the hard drive of the host computer as 512 by 512 8-bit (256 gray levels) pixel image data. A DT-IRIS image software package was used to control the operation of the framegrabber. Figure 3.1 is a sketch of the physical layout of the experiment.

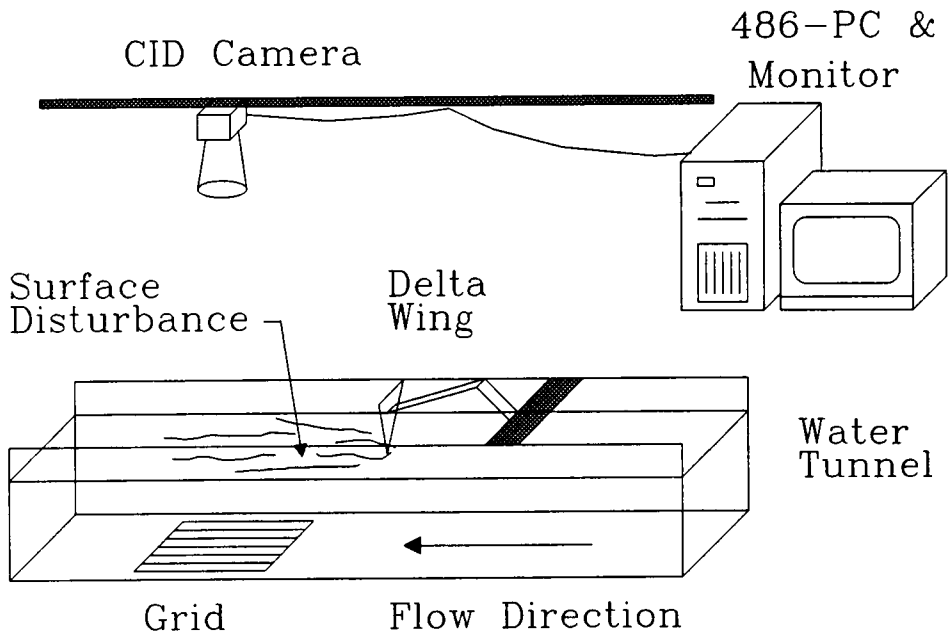


Figure 3.1 : Physical layout of the experiment.

Five different spatial cosine grids were used in this experiment to determine an optimal cosine frequency for the grid. These cosine grids were computer generated in order to approximate a true gray level cosine as closely as possible. Previous attempts using hand drawn line patterns yielded unsatisfactory results due to the abrupt transitions between the black and white lines. These early grids more

closely resembled square waves which introduced higher frequency harmonics into the images making them difficult to filter.

The program used to generate the cosine grids allowed a user-specified period in pixels of the cosine pattern as an input. A spatially varying cosine waveform was then generated and displayed on a monitor. A photograph of the grid was then taken using a graphics film recorder. The pictures were developed and enlarged to be used under the water tunnel. The dimensions of the grids/photos were 28 cm by 36 cm. It is important to note that the user-specified spatial frequency for the cosine grid was that of the original discrete grid at the time it was generated and first displayed. The final spatial frequency that was observed during the experiment (in the reference image) was a result of enlarging and printing the pictures (or grids) and the focusing parameters of the camera and lens. The five different spatial cosine frequencies which were designed and used in this experiment were 2.5, 1.45, 1.04, 0.93, and 0.83 cycles per cm resulting in normalized frequencies of 0.112, 0.066, 0.049, 0.043, and 0.038 cycles per pixel respectively in the acquired digital images.

Two different types of surface disturbance data were recorded. The first type was water droplet data. A droplet of water was released into a completely still and non-moving water surface. The ripple effects of the droplet on the surface were recorded as they passed through the viewing area of the camera and before they reflected off the side walls of the tunnel. Four frames were recorded for each of the three cosine grids with spatial frequencies of 2.5, 1.45, and 0.93 cycles per cm.

The second type of disturbance data was the surface wake data. The tip of

a delta wing was allowed to penetrate the surface of the flow just upstream of the camera viewing area. This generated a surface wake disturbance which was then observed and recorded. Three different water velocities were used to increase the amount of disturbance at the surface. Two frames were taken of the disturbed flow at each velocity level. This was done for all five spatial cosine grids.

Each time a new grid was fastened to the bottom of the tunnel, a new reference image was taken of that particular grid. The flow was stopped and the surface held completely still when the reference image was acquired. After the reference image was acquired, the camera configuration could not be changed or disturbed until all of the data that was needed using that particular grid and configuration had been recorded. If the camera configuration was disturbed in any manner, a new reference image had to be recorded. This was because the data being recorded was spatial or position dependent. If there was a positional discrepancy between the data and reference images, the cross-multiplication process would yield faulty results. Therefore it was crucial that once a grid had been affixed to the bottom of the tunnel and the reference image recorded the camera and lens configuration not be disturbed.

Reconstruction Method

After the data had been acquired in the water tunnel facility, it was taken and processed according to the theory discussed in Chapter II. The first objective was to cross-multiply the reference image (undisturbed water surface) and the data image

(disturbed water surface). The DT-IRIS image software package and related programs were used to load the reference and data images into two separate image buffers. The constant background intensity (dc value) was removed by calculating the average value of the pixels in each row and then subtracting it from each individual pixel value. Each row of the reference image was then multiplied pixel by pixel with the corresponding row in the data image. The pixel values were scaled by a factor of 2/127 and added to a constant value of 127 in order to keep the cross-multiplied values within the full-scale pixel value range (0 to 255). The cross-multiplied data was then stored in a third image buffer. This procedure was repeated for all 512 rows in the image. A listing of the FORTRAN code used to perform this procedure is given in Appendix A.

The second step in the reconstruction process was the filter design. A different digital filter was required for each of the five cosine grids used. The cutoff frequencies for the filters were determined experimentally by measuring the carrier frequencies of the reference images for each of the grids. These carrier frequencies were used as the first iterations for the transition band specifications in the filter design. An optimal transition band was then experimentally determined for each of the filters. In each case a 101 tap filter was designed to minimize the transition bandwidth of the filter and still achieve a -48 dB (equal to 1/256 as discussed in Chapter II under Filter Design) rejection rate in the stopband. The width of the transition band varied for the different filters. An FIR software package [18] was used to perform the design iterations using the Parks-McClellan program. Five

optimal FIR equiripple filters were designed (one for each grid) using this procedure. The final filter specifications for each cosine grid are given in Table 3.1.

Table 3.1 : Final filter specifications for each of the grids listed.

FILTER	BAND	BANDWIDTH	DEVIATION (dB)
2.5 cycle/cm Grid	Passband	0.0 - 0.055	0.03387
	Stopband	0.08 - 0.5	-48.163
1.45 cycle/cm Grid	Passband	0.0 - 0.039	0.03299
	Stopband	0.065 - 0.5	-48.391
1.04 cycle/cm Grid	Passband	0.0 - 0.022	0.03917
	Stopband	0.0467 - 0.5	-46.898
0.93 cycle/cm Grid	Passband	0.0 - 0.017	0.03368
	Stopband	0.0427 - 0.5	-48.213
0.83 cycle/cm Grid	Passband	0.0 - 0.014	0.03379
	Stopband	0.0385 - 0.5	-48.185

A program was written to filter the cross-multiplied image one row at a time using discrete Fourier transform (DFT) processing. The first 51 filter coefficients were read in starting with the center coefficient. Then 411 zeros were added to pad the filter length, and the remaining 50 filter coefficients were attached in reverse order of the first 51 excluding the first coefficient. This accomplished the impulse response shifting discussed in Chapter II which resulted in a zero phase response FIR filter. The filter coefficient array thus had 411 zeros and 101 nonzero coefficients for a total of 512 values.

Instead of convolving in the spatial domain, the filtering was accomplished by multiplying in the frequency domain. In order to do this a 512 point fast Fourier transform (FFT) was taken of both the filter coefficient array (hence the need for the zero padding) and of each row in the data image. The FFT data of each were then multiplied by the other pixel by pixel. The inverse fast Fourier transform (IFFT) was then taken of the multiplied FFT data to convert the information back into the spatial domain. This filtered data was then stored in a fourth image buffer. The filtering process was repeated for each row in the cross-multiplied image. The first and last 50 pixels in each row of the image were corrupted due to the circular convolution effects. A listing of the FORTRAN code for this program is given in Appendix B.

The rows of filtered data were reconstructed into an image and displayed. Image enhancement techniques were then used to improve the resolution of the images. The primary objective was to enhance the contrast of the image. Histogram equalization and contrast stretching were both used; however, the latter yielded better control of the modification and better subjective results. Histogram equalization [16,17] is a popular method of image enhancement. The goal of the technique is to equalize the histogram of the gray levels in the image so that the histogram is uniform. The result is a grayscale image which has an equal number of pixels of all the gray levels present in the image. Contrast stretching is simply a linear mapping of a specified gray level range to the full gray level scale. If all of the desired information in an image is contained in a set gray level region, this

region can be stretched to provide greater contrast of the information. This type of subjective image enhancement or modification was performed on the filtered data images.

A general block diagram of the reconstruction process is presented in Figure 3.2.

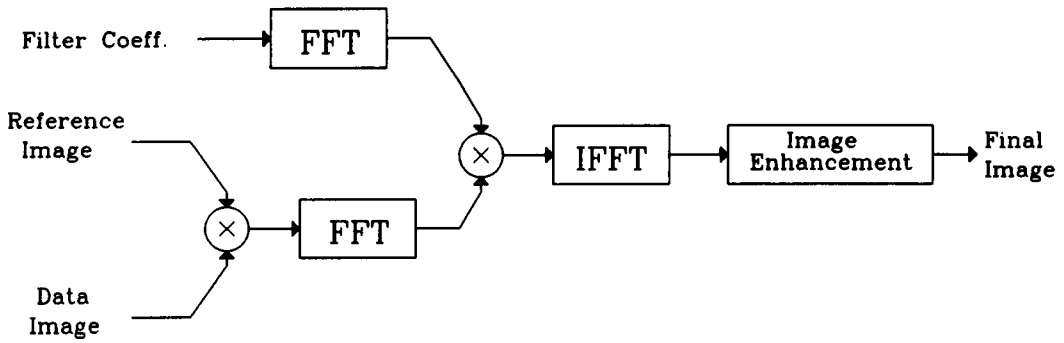


Figure 3.2 : General block diagram of the reconstruction process.

In summary, the data images were spatially multiplied with the corresponding reference images. The resulting images were then filtered with the appropriate FIR zero phase equiripple filters using frequency domain methods. The filtered images were then enhanced by means of contrast stretching and histogram equalization. The final images detailed in grayscale format the location, general outline, and intensity of the free surface turbulence.

CHAPTER IV

RESULTS AND ANALYSIS

The results of the experimental work described in Chapter III are presented in this chapter. The first section describes the results realized at each intermediate stage of the reconstruction process using the water droplet surface disturbance data. The second section presents the final images and results of the wake flow surface disturbance. The sections include some discussion and comparison of the contents of the various images obtained and the different spatial cosine grids used.

Water Droplet Data

Figure 4.1 is an example of the format and content of the reference images used in the reconstruction process. This particular reference image was taken of the spatial cosine grid with a frequency of 2.5 cycles per cm. Figures 4.1 through 4.8 each had a field of view of approximately 26 cm by 32 cm. Figure 4.2 is a photograph of a corresponding data image where the surface disturbance is visible as the warped or distorted lines of the spatial cosine grid. As was the case in the reference image of Figure 4.1, this data image was taken using the grid with a 2.5 cycle per cm spatial cosine frequency. The surface disturbance was generated using a single droplet of water as discussed in Chapter III and the data image acquired approximately 0.5 seconds after impact. The result of the cross-multiplication of these reference and data images is shown in Figure 4.3. It is obvious from this

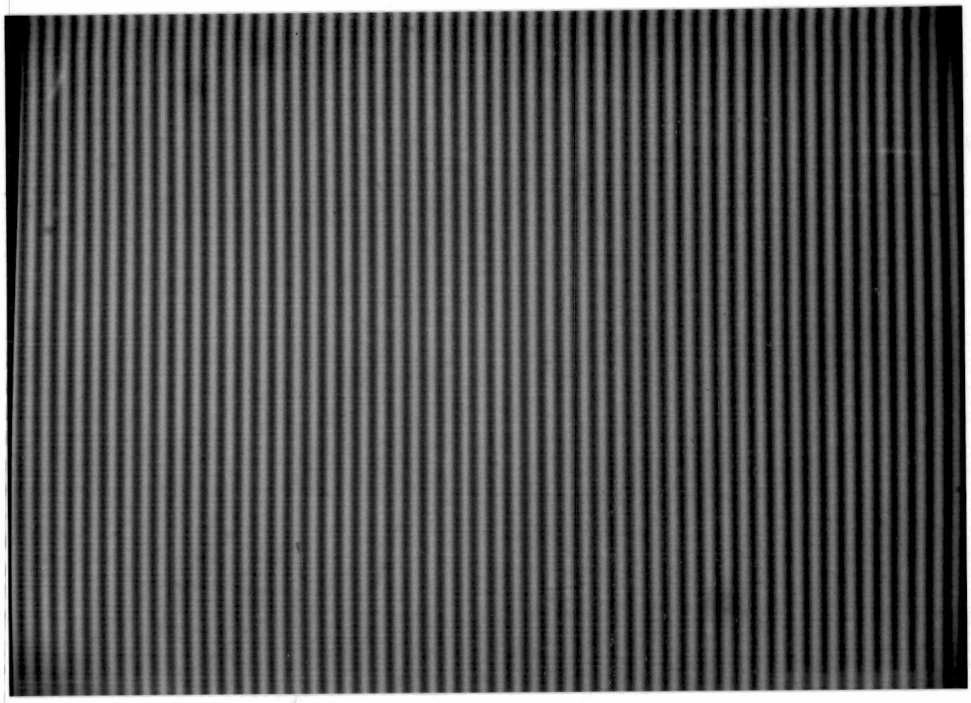


Figure 4.1 : Reference image using a 2.5 cycle/cm cosine grid.

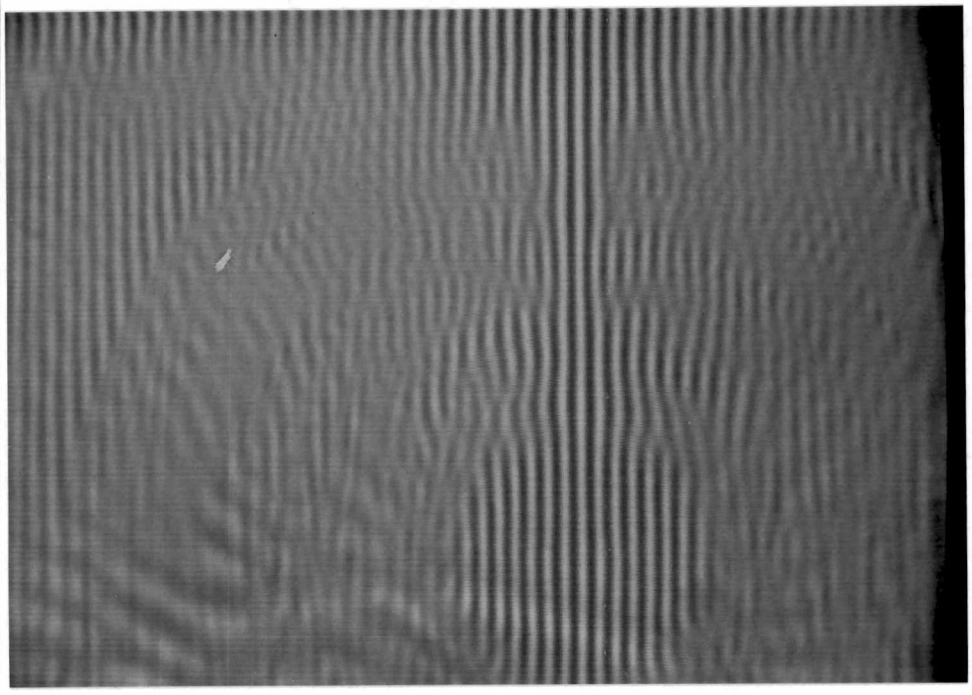


Figure 4.2 : Data image of a water droplet using a 2.5 cycle/cm cosine grid.

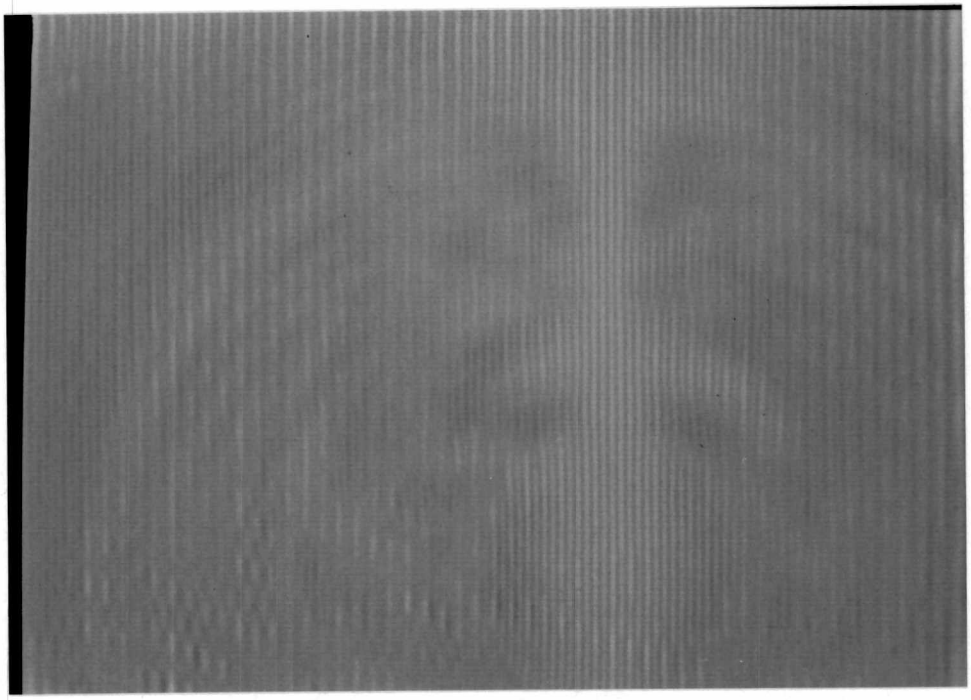


Figure 4.3 : Cross-multiplication of the reference image (Figure 4.1) and the data image (Figure 4.2).

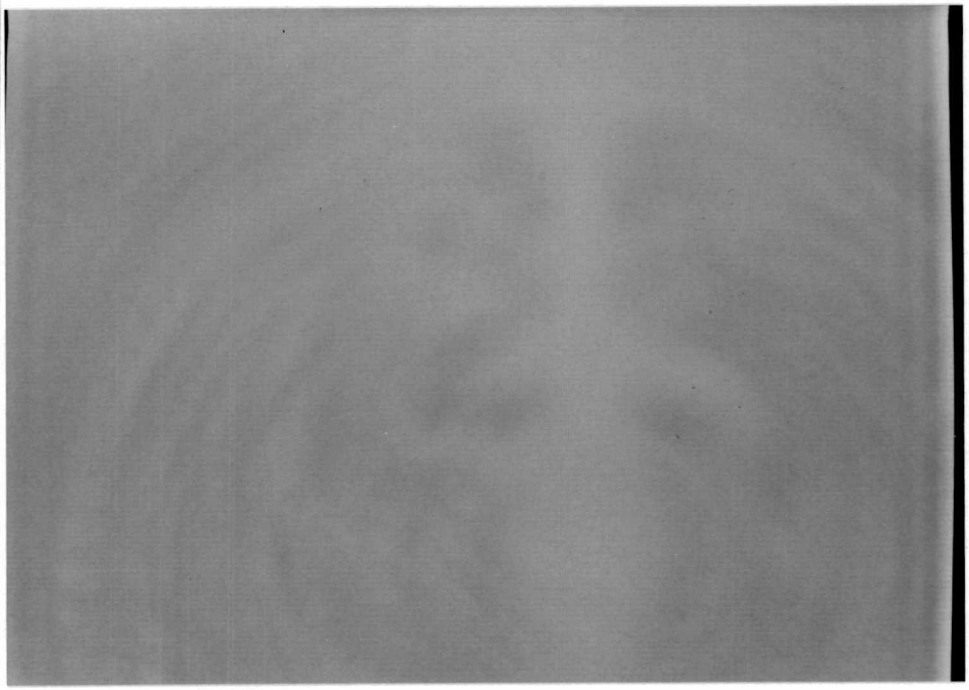


Figure 4.4 : The filtered cross-multiplication image in Figure 4.3.

image that the cross-multiplied data contains a cosine waveform which has double the frequency of the original grid.

The image in Figure 4.4 shows the cross-multiplied data after having been filtered with the appropriate filter. The carrier cosine has almost completely been rejected in the filter process. It is difficult to recognize the contents of this image as being representative of the surface disturbance due to the lack of contrast. Figure 4.5 shows the same image after contrast stretching the pixel region between values of 110 and 140 to the full pixel value range (0 to 255). The surface disturbance becomes very evident as a pattern of rings emanating out from the bottom of this final enhanced image.

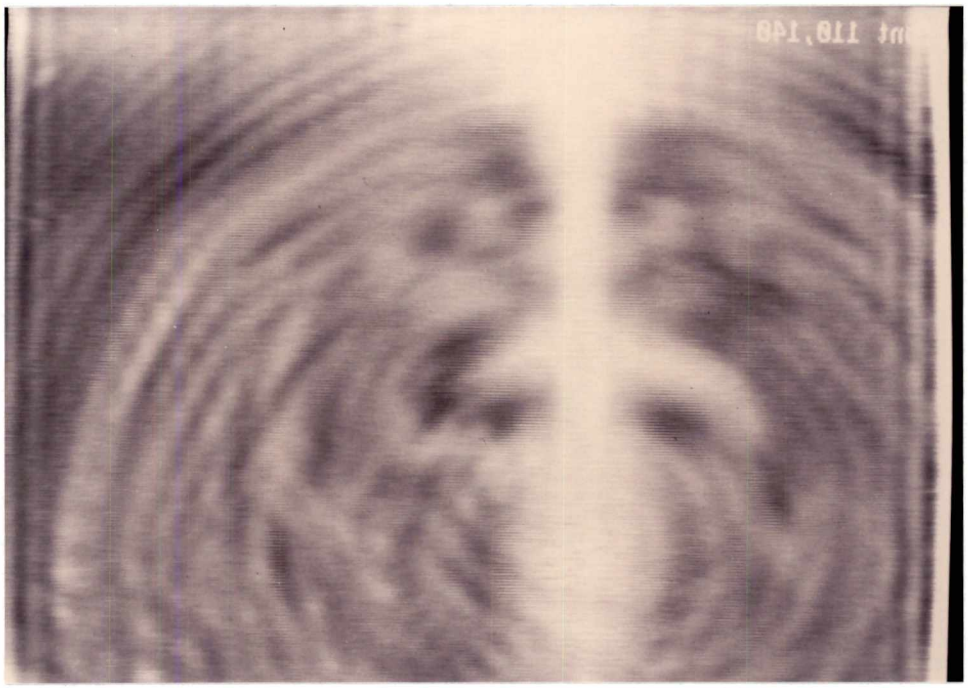


Figure 4.5 : Filtered image after contrast stretching (110 to 140).

A couple of interesting remarks can be made about the information in Figure 4.5. First, this reconstruction method gives an accurate visualization of what the surface disturbance pattern really is. The pattern of rings that is visible in this image is exactly what would be expected from a water droplet interacting with a still water surface. Secondly, there is some loss of information when the surface disturbance has a gradient which is perpendicular to the direction of the spatial cosine grid. This is recognized in the final enhanced image by the high intensity line which travels through the center of the image. The explanation for this phenomena is that no phase shift was introduced into the lines of the cosine grid by the surface disturbance for this region of the surface disturbance. A quick glance at the original data frame (Figure 4.2) confirms the fact that the cosine lines in the center of the image contain no modulation from the surface. They are almost completely straight when compared with the other lines in the data image.

Thirdly, there appears to be hints of a cosine grid still visible in the image which increases in intensity at the edges of the image. These grid lines which appear at the edges of the image are due to the circular convolution effects present in these points. There is a band of 50 pixels wide (which corresponds to approximately half the impulse response length) on each side of the image which is not completely filtered due to the nature of the filter operation. Finally, the image enhancement process of contrast stretching allowed a much better subjective analysis of the image. Since only a section of the pixel range was stretched, some pixel values were clipped. As a result, the final enhanced image (Figure 4.5) actually lost

some information. However, the information which is present is much more visible than in the unenhanced image (Figure 4.4).

Wake Flow Surface Disturbance

The previous section provided results at each stage of the reconstruction process and discussed the various aspects of the final enhanced images using the water droplet data. This section presents the analysis and discussion of the various grid designs using the wake flow surface data. The direction of the water flow as seen in the following figures is from the bottom of the image to the top.

Figure 4.6 is an enhanced image of the wake surface disturbance using a spatial cosine grid with a 2.5 cycle per cm carrier frequency. The image has been contrast stretched between the pixel values of 115 and 150. The surface disturbance is rather intricate in this frame and yet the image resulted in a surface outline which is rather clear and defined. Figure 4.7 is a contrast stretched image (between pixel values 110 and 160) of the wake surface flow with the same type of extreme disturbance using a cosine grid with a 1.04 cycle per cm frequency.

A clear degeneration of definition is evident between the higher and lower frequency grids, where the free surface details visualized using the lower frequency grids are somewhat less defined. The contrast stretched image (between pixels values 100 and 170) in Figure 4.8 of the wake surface flow, where the data image was acquired under similar complex surface disturbance conditions with an even lower frequency cosine grid (0.083 cycles per cm), confirms the trend. The

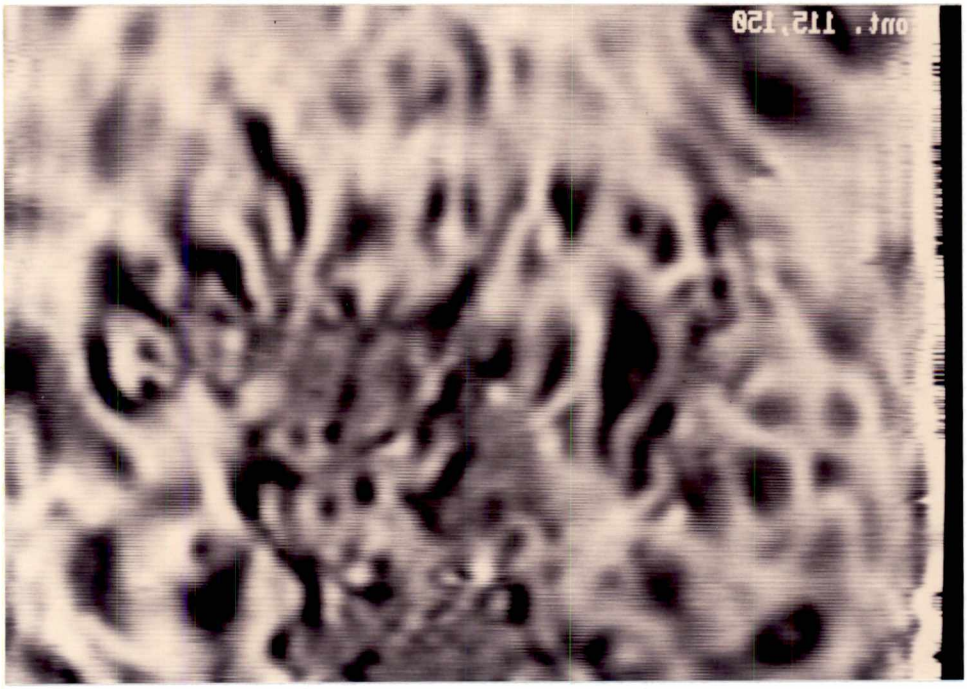


Figure 4.6 : Wave flow surface using a 2.5 cycle/cm cosine grid.

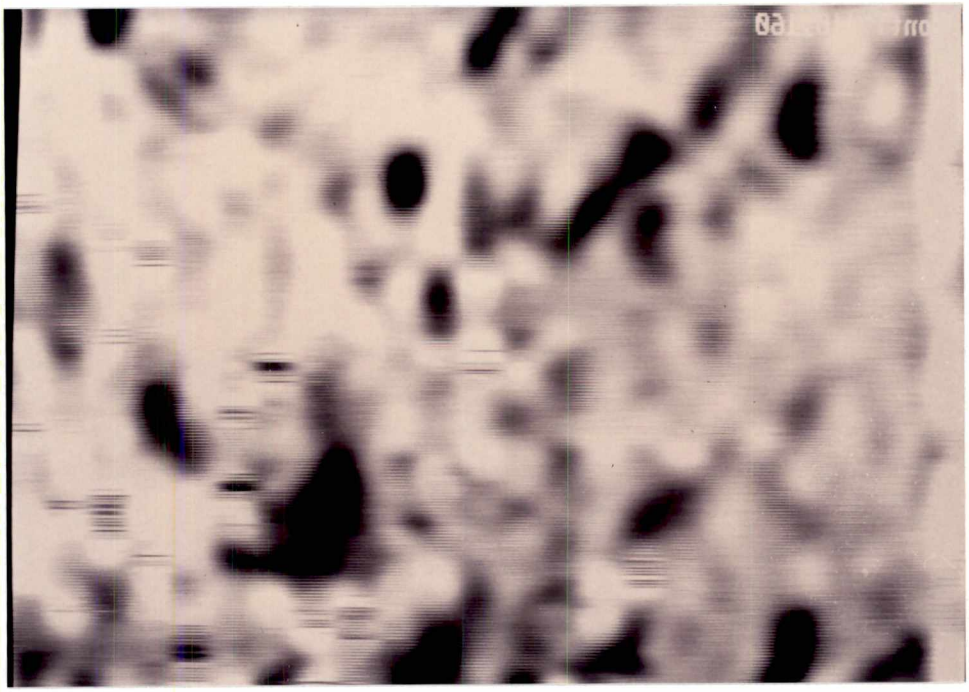


Figure 4.7 : Wake flow surface using a 1.04 cycle/cm cosine grid.

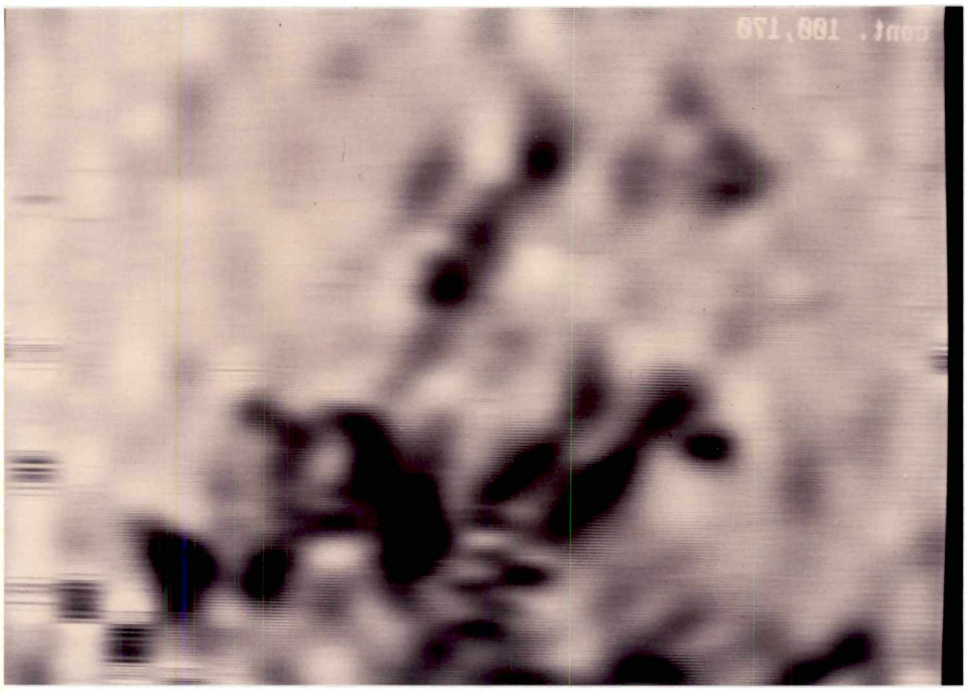


Figure 4.8 : Wake flow surface using a 0.83 cycle/cm cosine grid.

definition of the surface outline has decreased significantly in the cases where lower frequency cosine grids were used to collect the surface deformation data. The only advantage the lower frequency cosine grids might have over the higher frequency grids is the visualization of larger free surface waves and disturbance.

The images shown in Figures 4.6, 4.7, and 4.8 were all acquired using low amplitude surface disturbances. The data images would become distorted under extreme free surface disturbance conditions if higher frequency cosine grids were used. This is because of the possibility of breakup and crossing of the cosine lines in the acquired data images. Using lower frequency grids where the separation between the lines in the cosine is greater would allow larger and more severe surface

disturbance patterns to be visualized. However, details of the surface disturbance may be lost in the low pass filtering operation.

CHAPTER V

SUMMARY AND CONCLUSIONS

A new technique has been developed for the simple but effective visualization of mild free surface disturbances in a water tunnel. This method takes advantage of the refractive characteristics of water and uses image processing techniques to produce an image which details the outline, location, and extent of the free surface in a grayscale format. This is accomplished by acquiring images of a cosine grid as seen through the surface disturbance pattern, cross-multiplying them with reference images, and then filtering and enhancing the results.

The main advantage that this technique has over previous methods is that it requires a minimal amount of equipment and almost no calibration, and yet it provides high quality results. The Moire [6,9] method required the use of two identical high quality and carefully calibrated grids in order to achieve reasonable quantitative results. A number of the reflective methods [6,8,12] required special lighting and mirror configurations in order to visualize the desired flow characteristics. The method presented in this thesis requires no special lighting and can be implemented effectively using the rather simple experimental configuration described in Chapter III.

It was determined that data acquired with the higher frequency cosine grids yielded higher content definition of moderate surface disturbances than data acquired with lower frequency grids. Smaller deformations of the surface could be detected

using the higher frequency grids due to the closer line spacing of these grids. While data acquired using the lower frequency grids had less content definition, the lower frequency grids could be used for visualizing more severe free surface disturbances. The larger line spacing of these grids allowed for greater warping (or phase modulation) without the effects of breakup or line crossing. Of the five cosine grids tested, the grid with a spatial frequency of 2.5 cycles per cm (the highest frequency grid) yielded the best subjective results for the type of flow tested. However, the optimal cosine grid will depend on the particular application and the type of free surface information desired.

Zero phase equiripple FIR filters were designed to minimize the amount of distortion the filtering might add to the final image. Performing the filtering in the frequency domain allowed careful inspection of the frequency components and responses at each step in the reconstruction process. Larger filter orders could have been used to achieve smaller transition bands when filtering the lower frequency grids. However, the larger the impulse response of the filter, the greater the number of partially filtered points on the sides of the images. It was difficult to filter the data which was obtained using the low frequency grids without losing some of the high frequency information of the surface deformation. This made the lower frequency grids a lesser option in the cosine grid selection.

Further research should be conducted to determine the exact correlation between the intensity levels of the final grayscale image and the free surface deformation. If a correlation could be determined, maps of the free surface

disturbances could be generated and used in quantitative analysis of the free surface flow characteristics. Different grid patterns including circularly symmetric grids or angled cosine grids could be examined in an attempt to eliminate the "blind spot" of the current cosine grid as seen in the water droplet data.

BIBLIOGRAPHY

BIBLIOGRAPHY

[1] T. Sarpkaya, "Three-dimensional interactions of vortices with a free surface," AIAA paper No. 92-0059, Reno, Nevada, January 1992.

[2] T. Utami and T. Ueno, "Visualization and picture processing of turbulent flow," *Experiments in Fluids 2*, pp. 25-32, 1984.

[3] L. G. Blows and L H. Tanner, "A method for the measurement of fluid surface velocities, using particles and a laser light source," *Journal of Physics E: Scientific Instruments*, Volume 7, pp. 402-405, 1974.

[4] W. W. Willmarth, G. Tryggvason, A. Hirsa, and D. Yu, "Vortex pair generation and interaction with a free surface," *Physical Fluids*, Volume 1, No. 2, pp. 170-172, February 1989.

[5] A. D. Vakili and A. Gabrie, "Three-dimensional surface deformation measurements of an incompressible flow using active image reconstruction," 12th U.S. National Congress of Applied Mechanics, Seattle, Washington, June 27 - July 1, 1994.

[6] I. Grant, I. Padilla, and N. Stewart, "Measurement of water surface elevation using Moire techniques," Conference on Offshore Mechanics and Arctic Engineering, The Hague, Netherlands, pp. 547-552, March 1989.

[7] B. L. Gotwols and G. B. Irani, "Charge-coupled device camera system for remotely measuring the dynamics of ocean waves," *Applied Optics*, Volume 21, No. 5, pp. 851-860, March 1982.

[8] D. Dabiri, X. Zhang, and M. Gharib, "A real-time free-surface elevation mapping technique," Submitted to the Seventh International Symposium on Applications of Laser Techniques to Fluid Mechanics, Lisbon, Portugal, July 1994.

[9] A. Mizuno, Y. Nagase, and K. Yamauchi, "K.-Moire method: a technique for visualizing slightly deformed liquid surface," Kogakuin University, Tokyo, Japan, pp. 663-668.

[10] C. S. Cox, "Measurements of Slopes of High-Frequency Wind Waves," *Journal of Marine Research*, Volume 16, p. 199, 1958.

[11] F. Y. Sorrel and A. L. Withers, "Optical technique for measurement of random water wave surfaces," *Review of Scientific Instruments*, Volume 47, No. 12, pp. 1445-1449, December 1976.

[12] T. Sarpkaya and D. O. Henderson Jr., "Free surface scars and striations due to trailing vortices generated by a submerged lifting surface," AIAA paper No. 85-0445, Reno, Nevada, January 1986.

[13] L. Montgomery Smith, *Fundamental Principles of Optical Engineering*, Tullahoma, Tennessee, preprint, pp. 64 and 84, 1994.

[14] J. P. Proakis and D. G. Manolakis, *Digital Signal Processing*, Macmillan, New York, 1992.

[15] B. Bomar and L. M. Smith, "Digital signal processing for instrumentation and data analysis," University of Tennessee, ECE Department, March 1993.

[16] T. S. Huang, "Picture processing and digital filtering," *Topics in Applied Physics*, Volume 6, 1979.

[17] R. Gonzalez and R. Woods, *Digital Image Processing*, Addison-Wesley, Reading, Massachusetts, 1992.

[18] B. Bomar, *IIR & FIR Digital Filter Design Software*, Version 1.2, Tullahoma, Tennessee, 1989.

APPENDIXES

APPENDIX A

```
C-----PROGRAM    CROSMULT.FOR-----------------------------------------------------
C
C       Program 1.0
C       July 16, 1993
C       Doug Britton
C
C-------------------------------------------------------------------------------------
C
C       The purpose of this program is to digitize two images containing
C       sinusoidal information, and then to perform a cross multiplication
C       of the two images row by row. The principle being used is based
C       upon a couple of assumptions. It is assumed that one of the 2
C       images is a simple cosine wave. The other image is assumed to be
C       a cosine wave with a simple phase distortion. The first image
C       (Stil) is a picture of the grid on the bottom of the water tunnel
C       with no surface disturbance. The second image (Move) is a picture
C       of the grid on the bottom of the water tunnel as reflected through
C       the disturbed surface pattern. The cross multiplication results as
C       follows:
C           Stil = Cos[w(t)]
C           Move = Cos[w(t)+q(t)]    where q(t) is the phase distortion
C
C           Cos[w(t)]*Cos[w(t)+q(t)] = 0.5*Cos[q(t)] + 0.5*Cos[2*w(t)+q(t)]
C
C       If the resulting information is lowpass filtered, the phase
C       distortion information can be retrieved and regenerated as an image.
C
C-----MAIN    PROGRAM-----------------------------------------------------------

      PROGRAM CROSMULT
      IMPLICIT NONE

$STORAGE:2
$INCLUDE:'C:\IRIS\ISDEFS.FOR'

C-----VARIABLE/CONSTANT    DECLARATION-----------------------------------

      INTEGER*2  I
      INTEGER*2  STILBUFF
      INTEGER*2  MOVEBUFF
```

```
      INTEGER*2  OUTBUFF
      INTEGER*2  STATUS
      INTEGER*2  ROW
      INTEGER*2  COL
      INTEGER*2  LN
      INTEGER*2  N
      PARAMETER  (LN = 9)        !2**ln = the N in an N x N image
      PARAMETER  (N = 2**LN)     !N is an N x N image.
      INTEGER*2  STIL(N)
      INTEGER*2  MOVE(N)
      INTEGER*2  OUT(N)

      REAL*4     TEMP
      REAL       AVSTIL
      REAL       AVMOVE
      CHARACTER*40 OUTFILE

C-----VARIABLE    INITIALIZATION----------------------------------------------------

      ROW = 0                    !Setting default row position to 0
      COL = 0                    !Setting default col position to 0

      WRITE(*,*) 'ENTER INPUT BUFFER FOR THE STILL IMAGE =>'
      READ(*,*) STILBUFF
      WRITE(*,*) 'ENTER INPUT BUFFER FOR THE MOVING IMAGE =>'
      READ(*,*) MOVEBUFF
      WRITE(*,*) 'ENTER THE BUFFER FOR THE RESULTING IMAGE =>'
      READ(*,*) OUTBUFF
C
      STATUS = ISINIT()
      STATUS = ISDISP(1)             !1 enables display, 0 disables display
      STATUS = ISOTFR(OUTBUFF)       !Selects output frame buffer (BUFF)
                                     !Turn on the cursor
      STATUS = ISCURS(1)             !1 enables cursor, 0 disables cursor

C-----CAPTURE    PIXEL    VALUES-----------------------------------------------------

      DO ROW = 0, N-1
         COL = 0
         STATUS= ISCPOS(ROW,COL)
         STATUS = ISGETP(STILBUFF,ROW,COL,N,STIL)
         STATUS = ISGETP(MOVEBUFF,ROW,COL,N,MOVE)
         AVSTIL = 0.0
```

```
            AVMOVE = 0.0
            DO I=1,N
               AVSTIL = AVSTIL + FLOAT(STIL(I))
               AVMOVE = AVMOVE + FLOAT(MOVE(I))
            END DO
            AVSTIL = AVSTIL/FLOAT(N)
            AVMOVE = AVMOVE/FLOAT(N)
            DO I = 1, N
               TEMP=(FLOAT(STIL(I))-AVSTIL)*
     &              (FLOAT(MOVE(I))-AVMOVE)
               TEMP = 2*TEMP/127
               OUT(I) = 127 + INT2(TEMP)
            END DO

            STATUS = ISPUTP(OUTBUFF,ROW,COL,N,OUT)

         END DO

C-----TURN    EVERYTHING    OFF-----------------------------------------------------

         STATUS = ISCURS(0)          !Turning off cursor
         STATUS = ISEND()            !Closing the IS_routines
         STOP

C-----END    OF    MAIN    PROGRAM-------------------------------------------------

         END
```

APPENDIX B

```
C-----PROGRAM    IMFILTER.FOR-----------------------------------------------------
C
C      Program 1.0
C      July 21, 1993
C      Doug Britton
C
C-------------------------------------------------------------------------------------
C
C      The purpose of this program is to convert a video image into the
C      one dimensional Fourier Transform using its gray scale values.
C      The process takes place on a row by row basis, where each row
C      contain N points (0 to N-1).
C
C      The FFT is also taken of the filter coefficients listed and the
C      data is filtered by multiplying the 2 FFT's (one of the data,
C      and one of the filter coefficients).
C
C          Y(w) = H(w)*X(w)
C
C      Then the IFFT is taken to reconstruct the image.
C
C      Before the FFT can be taken, a lookup table must be generated
C      using the subroutine INIT.FOR.
C
C      DAT = COMPLEX ARRAY FOR IMAGE INPUT DATA
C      F = COMPLEX ARRAY FOR FFT INPUT DATA
C      FCOEF = COMPLEX ARRAY FOR FFT COEF. DATA
C      W = COMPLEX ARRAY FOR TWIDDLE FACTORS
C      LN = REAL VARIABLE LN = Log2 N  OR N = 2**LN
C
C-----MAIN    PROGRAM---------------------------------------------------------------

      PROGRAM IMFILTER
      IMPLICIT NONE

$STORAGE:2
$INCLUDE:'C:\IRIS\ISDEFS.FOR'

C-----VARIABLE/CONSTANT    DECLARATION-----------------------------------

      INTEGER*2  I
```

```
      INTEGER*2  INBUFF
      INTEGER*2  OUTBUFF
      INTEGER*2  STATUS
      INTEGER*2  ROW
      INTEGER*2  COL
      INTEGER*2  LN
      INTEGER*2  LM
      INTEGER*2  N              !N is the length of the data record
      INTEGER*2  M              !M is the number of filter coeff.
      INTEGER*2  MACT           !MACT is number of filter coeff in data file
      INTEGER*2  ITEMP
      PARAMETER  (LN = 9)       !2**ln = the N in an N x N image
      PARAMETER  (N = 2**LN)
      INTEGER*2  PIXEL(N)
      INTEGER*4  HIST(256)

      REAL       RTEMP
      COMPLEX    F(N)
      COMPLEX    FCOEF(N)
      COMPLEX    W(N)
      COMPLEX    V(N)
      CHARACTER*40 OUTFILE
      CHARACTER*40 HISTFILE
      CHARACTER*40 COEFFILE
      CHARACTER*1  ANS

C-----VARIABLE     INITIALIZATION----------------------------------------------

      ROW = 0                   !Setting default row position to 0
      COL = 0                   !Setting default col position to 0

      WRITE(*,*) 'ENTER INPUT BUFFER =>'
      READ(*,*) INBUFF
      WRITE(*,*) 'ENTER OUTPUT BUFFER =>'
      READ(*,*) OUTBUFF

      STATUS = ISINIT()
      STATUS = ISDISP(1)            !1 enables display, 0 disables display
      STATUS = ISOTFR(OUTBUFF)      !Selects output frame buffer (BUFF)
                                    !Turn on the cursor
      STATUS = ISCURS(1)            !1 enables cursor, 0 disables cursor

C-----OPEN   STORAGE   FILE---------------------------------------------------
```

```
      WRITE(*,*)'ENTER NAME OF FILTER COEFFICIENT FILE =>'
      READ(*,'(A)') COEFFILE
      OUTFILE = COEFFILE
      COEFFILE = 'D:\DOUG\DSP\'//OUTFILE
      WRITE(*,'(A)') COEFFILE

C-----SET  UP  LOOK-UP  TABLE  INIT.FOR----------------------------------
      CALL INIT(W, LN, N)

C-----OPEN  &  READ  FILTER  COEFFICIENTS---------------------------
      OPEN (UNIT=20, STATUS='UNKNOWN', FILE=COEFFILE)
      REWIND 20

      READ(20,100) M
      READ(20,100) MACT
      READ(20,100) ITEMP
100   FORMAT(I20)

      WRITE(*,*) M
      WRITE(*,*) MACT

      DO I=1,N
         F(I) = (0.0,0.0)
         FCOEF(I) = (0.0,0.0)
      END DO

      DO I= 1,MACT-1
         READ(20,110) RTEMP
         FCOEF(N-MACT+1+I) = CMPLX(RTEMP,0.0)
         FCOEF(MACT+1-I) = CMPLX(RTEMP,0.0)
      END DO

      READ(20,110) RTEMP
      FCOEF(1) = CMPLX(RTEMP,0.0)
110   FORMAT(E25.8E4)

      CLOSE(20)

C-----GENERATE  FILTER  COEFFICIENT  FFT-------------------------------

      CALL FFT(FCOEF, W, LN, N)

C-----GENERATE  DATA FFT,  FILTER,  GENERATE  IFFT----------
```

```
      DO ROW = 0,N-1
         COL = 0
         STATUS = ISCPOS(ROW,COL)
         STATUS = ISGETP(INBUFF,ROW,COL,N,PIXEL)

      DO I=1,N
         F(I) = CMPLX(PIXEL(I),0.0)
      END DO

      CALL FFT(F, W, LN, N)

      DO I=1,N
         F(I) = FCOEF(I)*F(I)
      END DO

      CALL IFFT(F, W, LN, N)

      DO I=1,N
         RTEMP = CABS(F(I))
         PIXEL(I) = INT(RTEMP) + 127
      END DO

      STATUS = ISPUTP(OUTBUFF,ROW,COL,N,PIXEL)

      END DO

C-----TAKE   HISTOGRAM   OF   IMAGE----------------------------------------

      WRITE(*,*)'DO YOU WANT A HISTOGRAM ?(Y/N) =>'
      READ(*,'(A)') ANS
      IF (ANS.EQ.'N') THEN
         GOTO 8000
      ELSEIF (ANS.EQ.'n') THEN
         GOTO 8000
      ENDIF

      STATUS = ISHIST(OUTBUFF, HIST)

      WRITE(*,*) 'ENTER NAME OF HISTOGRAM FILE =>'
      READ(*,'(A)') HISTFILE
      OPEN (UNIT=30, STATUS='UNKNOWN', FILE=HISTFILE)
      REWIND 30
```

```
      DO I=1,256
         WRITE(30,100) HIST(I)
      END DO

      CLOSE(30)

C-----TURN   EVERYTHING   OFF----------------------------------------------------

8000  STATUS = ISCURS(0)          !Turning off cursor
      STATUS = ISEND()               !Closing the IS_routines
      END

C-----END   OF   MAIN   PROGRAM------------------------------------------------

C-----FFT   SUBROUTINE---------------------------------------------------------
      SUBROUTINE FFT(F, W, LN, N)

      INTEGER*2  LN
      INTEGER*2  N
      COMPLEX    F(N)
      COMPLEX    W(N)
      COMPLEX    T

      NV2 = N/2
      NM1 = N - 1

C-----REORDER   DATA-----------------------------------------------------------

      J = 1
      DO I = 1, NM1
         IF(I.GE.J) GOTO 1
            T = F(J)
            F(J) = F(I)
            F(I) = T
1        CONTINUE
         K = NV2
2        CONTINUE
         IF(K.GE.J) GOTO 3
            J = J - K
            K = K/2
         GOTO 2
3        CONTINUE
         J = J + K
```

```
      END DO

C-----MAIN   FFT   BUTTERFLY   LOOPS----------------------------------------

      DO  K = 1, LN
         LE = 2**K
         LE1 = LE/2
         NM1 = 1
         DO J = 1, LE1
            DO I = J, N, LE
               IP = I + LE1
               T = F(IP)*W(NM1)
               F(IP) = F(I) - T
               F(I) = F(I) + T
            END DO
            NM1 = NM1 + N/LE
         END DO
      END DO

C-----DIVIDE   BY   N--------------------------------------------------------------
      DO I = 1, N
         F(I) = F(I)/FLOAT(N)
      END DO

      RETURN
      END

C-----END   OF   FFT   SUBROUTINE-------------------------------------------
C-----SUBROUTINE   INIT-----------------------------------------------------------
      SUBROUTINE INIT(W, LN, N)

      INTEGER*2  N
      COMPLEX    W(N)
      COMPLEX    CMPLX

      P = 6.2831853071/FLOAT(N)

      DO I = 1, N
         A = P*FLOAT(I-1)
         W(I) = CMPLX(COS(A), -SIN(A))
      END DO
      RETURN
      END
```

```
C------SUBROUTINE    IFFT    (IFFT2.FOR)-----------------------------------------

      SUBROUTINE IFFT(F, W, LN, N)

      COMPLEX   F(N)
      COMPLEX   W(N)
      COMPLEX   T
      INTEGER*2 LN
      INTEGER*2 N

      NV2 = N/2
      NM1 = N - 1

C-----REORDER    DATA-----------------------------------------------------------
      J = 1
      DO I = 1, NM1
         IF(I.GE.J) GOTO 15
            T = F(J)
            F(J) = F(I)
            F(I) = T
15       CONTINUE
         K = NV2
25       CONTINUE
         IF(K.GE.J) GOTO 35
            J = J - K
            K = K/2
         GOTO 25
35       CONTINUE
         J = J + K
      END DO

C-----MAIN    IFFT    BUTTERFLY     LOOPS----------------------------------------

      DO  K = 1, LN
         LE = 2**K
         LE1 = LE/2
         NM1 = 1
         DO  J = 1, LE1
            DO  I = J, N, LE
               IP = I + LE1
               T = F(IP)*CONJG(W(NM1))
               F(IP) = F(I) - T
               F(I) = F(I) + T
```

```
            END DO
            NM1 = NM1 + N/LE
         END DO
      END DO

C-----MULTIPLY    BY    N-----------------------------------------------------------

      DO I=1,N
         F(I) = F(I)*FLOAT(N)
      END DO

      RETURN
      END

C-----END    OF    IFFT2    SUBROUTINE----------------------------------------
```

VITA

Douglas F. Britton was born in Bonaire, Netherland Antilles, on February 19, 1970. He attended the Dutch public Queen Beatrix Elementary School and graduated high school from the Black Forest Academy in Kandern, Germany, in 1988. He attended LeTourneau University in Longview, Texas, from September 1988 to May 1992, graduating with a Bachelor of Science degree in Electrical Engineering. In September of 1992 he entered the University of Tennessee Space Institute in Tullahoma, Tennessee, where he received a Master of Science degree in Electrical Engineering in May of 1994. He is currently in the process of enrolling in the Georgia Institute of Technology in Atlanta, Georgia.